Photoabsorption in molecular nitrogen: A moment analysis of discrete-basis-set calculations in the static-exchange approximation[a)]

T. N. Rescigno and C. F. Bender

Theoretical Atomic and Molecular Physics Group, University of California, Lawrence Livermore Laboratory, Livermore, California 94550

B. V. McKoy[b)]

Arthur Amos Noyes Laboratory of Chemical Physics, California Institute of Technology, Pasadena, California 91125

P. W. Langhoff[c)]

Department of Chemistry, Indiana University, Bloomington, Indiana 47401 and Joint Institute for Laboratory Astrophysics, National Bureau of Standards and University of Colorado, Boulder, Colorado 80309

(Received 3 October 1977)

Theoretical investigations of photoexcitation and ionization cross sections in molecular nitrogen are reported employing the recently devised Stieltjes–Tchebycheff moment-theory technique in the static-exchange approximation. The coupled-channel equations for photoabsorption are separated approximately by identifying the important physically distinct excitation processes associated with formation of the three lowest electronic states of the parent molecular ion. Approximate Rydberg series and pseudospectra of transition frequencies and oscillator strengths are constructed for the seven individual channel components identified using Hartree–Fock ionic core functions and normalizable Gaussian orbitals to describe the photoexcited and ejected electrons. Detailed comparisons of the theoretically determined discrete excitation series with available spectral data indicate general accord between the calculated and observed excitation frequencies and oscillator strengths, although there are some discrepancies and certain Rydberg series have apparently not yet been identified in the measured spectra. The total Stieltjes–Tchebycheff vertical photoionization cross section obtained from the discrete pseudospectra is in excellent agreement with recent electron–ion coincidence measurement of the cross section for parent–ion production from threshold to 50 eV excitation energy. Similarly, the calculated vertical partial cross sections for the production of the three lowest electronic states in the parent molecular ion are in excellent accord with the results of recent electron–electron coincidence and synchrotron–radiation branching ratio measurements. The origins of particularly intense resonancelike features in the discrete and continuum portions of the photoabsorption cross sections are discussed in terms of excitations into valencelike molecular orbitals. Small discrepancies between theory and experiment are attributed to specific autoionization processes and channel couplings not included in the calculations. In contrast to previously reported model or local potential studies, the present results employ the full nonlocal and nonspherical molecular Fock potential in *ab initio* photoabsorption calculations. The excellent agreement obtained between theory and experiment in molecular nitrogen suggests that highly reliable photoabsorption cross sections for diatomic molecules can be obtained from Hilbert space calculations and the Stieltjes–Tchebycheff method in the static-exchange approximation under appropriate conditions.

I. INTRODUCTION

The past two decades have witnessed significant improvements in techniques for measuring the photoabsorption cross sections of diatomic molecules.[1,2] In contrast to the experimental situation, precise *ab initio* photoabsorption calculations in molecules have been limited to the simplest diatomic systems,[3] primarily because of difficulties that arise in the construction of discrete many-electron eigenstates and continuum functions appropriate for the unbound motion of an ejected electron in the presence of a nonspherical ionic molecular core. Consequently, various computational simplifications, including the additive atomic approximation,[4] one-center many-body calculations,[5] the use of plane-wave final states,[6] the scattered-wave X_α method,[7] and the use of one- and two-center Coulomb wavefunctions,[8] have been employed in semiclassical photoabsorption calculations. Although certain of these techniques can be useful in specific cases, the introduction of simplifying approximations to the molecular potential and/or wavefunction can lead to cross sections of unknown quality.

In view of the difficulties that arise in computations of many-electron continuum eigenfunctions for diatomic molecules, various procedures have been suggested recently for constructing photoionization profiles employing the discrete oscillator strengths and transition frequencies obtained from variational calculations in Hilbert space,[9–11] techniques that have long proved useful in conventional bound-state configuration–interaction calculations.[12] Of the methods suggested, the Stieltjes–Tchebycheff technique,[10,11] based on theorems

[a)]This work was performed under the auspices of the U.S. Energy Research and Development Administration under contract No. W-7405-Eng-48.

[b)]Supported by a grant from the National Science Foundation.

[c)]JILA Visiting Fellow, 1976. Supported in part by the Donors of the Petroleum Research Fund, administered by the American Chemical Society.

 0021-9606/78/6803-0970$01.00

from the theory of moments,[13] has proved sufficiently flexible to accommodate the use of different types of basis functions, and to provide highly reliable results for both the discrete and continuum portions of photoabsorption profiles. In addition to illustrative calculations performed on one-electron model systems,[10,11] Stieltjes–Tchebycheff profiles have been reported for the negative hydrogen,[11b] lithium, sodium, and potassium ions,[14] atomic helium,[10c,11b] lithium,[15] and boron,[16] and molecular hydrogen[17] and formaldehyde,[18] and additional calculations are presently in progress on other atomic and molecular systems.[19]

A major advantage of L^2 scattering techniques, including the Stieltjes–Tchebycheff method, is that they rigorously avoid the need for explicit inclusion of asymptotic boundary conditions. This constitutes a significant advance in molecular scattering calculations, since the use of standard bound-state techniques allows the introduction of realistic molecular potentials. In particular, nonlocal exchange interactions can be treated without resorting to local approximations or parametrized model potentials.

In the present paper, the Stieltjes–Tchebycheff technique is employed in calculations of photoabsorption cross sections in molecular nitrogen. Excitation processes in nitrogen have been studied experimentally in considerable detail, due, in part, to a continuing aeronomic interest in its role as an atmospheric constituent.[1] Photoabsorption cross-section measurements employing conventional sources[20,21] have been supplemented with the use of synchrotron radiation[22] and the spectral assignments have been the subject of an extensive review.[23] Forward-scattering electron-impact-excitation spectra[24]—including the use of electron–ion coincidence techniques[25]—and photoelectron spectra[26] have been measured, and recent branching ratio studies employing conventional line sources,[21] electron–electron $(e, 2e)$ coincidence techniques,[27] and synchrotron radiation[28] have provided partial photoionization cross sections for the lowest ionic channels. Moreover, since there are three ionization thresholds in the ~15–19 eV excitation energy interval,[26] molecular nitrogen provides a useful test of the Stieltjes–Tchebycheff technique when applied to a relatively complex spectrum.

The coupled-channel equations for photoabsorption in molecular nitrogen are separated in the present study by identifying the important physically distinct excitation processes $[N_2(^1\Sigma_g^+) + h\nu \rightarrow N_2^+(X\,^2\Sigma_g^+,\ A\,^2\Pi_u,\ B\,^2\Sigma_u^+) + e^-]$ and decoupling them. Separate electronic variational calculations are carried out at the equilibrium internuclear separation for the seven-channel components identified employing ionic Hartree–Fock functions and basis sets of normalizable Gaussian functions for the photoexcited and ejected electrons. The seven calculated discrete excitation series obtained are compared with the available photoabsorption spectra,[20–23] and the origins of particularly intense resonances are discussed in terms of transitions into valencelike σ^* and π^* orbitals. Associated photoionization profiles are constructed employing the calculated pseudospectra of transition frequencies and oscillator strengths and the Stieltjes–Tchebycheff procedure. In this way, partial and total photoionization cross sections are obtained in the static-exchange approximation avoiding explicit use of molecular continuum eigenfunctions. In contrast to previously reported local or model potential studies,[7,8] the present results pertain to the solution of the Schrödinger equation for photoejected electrons in the full nonlocal and noncentral molecular Fock potential. The total Stieltjes–Tchebycheff vertical photoionization cross section obtained for the production of N_2^+ ions is in excellent agreement with the results of recent electron–ion coincidence measurements.[25] Similarly, the three computed partial cross sections are in good accord with the results of line source,[21] electron–electron coincidence,[27] and synchrotron radiation[28] branching-ratio measurements. The origins of resonancelike structures present in certain of the partial-channel cross sections are discussed in terms of excitations into valencelike orbitals in the continuum, and connection is made with alternative descriptions based on partial-wave expansions.[7] The present results suggest that reliable photoabsorption cross sections for diatomic molecules can be obtained from the Stieltjes–Tchebycheff method in the separated-channel static-exchange approximation under appropriate conditions.

The Stieltjes–Tchebycheff technique is briefly described in Sec. II, and a description of the channel-separation procedure is given in Sec. III. Computational methods employing Gaussian basis sets and the static-exchange approximation are described in Sec. IV. The numerical results obtained are presented and compared with experimental results in Sec. V. Section VI contains a summary and concluding remarks.

II. STIELTJES–TCHEBYCHEFF METHOD

The Stieltjes–Tchebycheff procedure has been described in considerable detail in previous publications.[10,11] Consequently, only those aspects of the development required for clarity are given here.

The strength of the interaction of a beam of unpolarized light with a target gas is conveniently described by the trace of the frequency-dependent polarizability tensor of the constituent molecules $\alpha(z)$ which can be written as a Stieltjes integral over the appropriate oscillator strength distribution in the form,[29]

$$\alpha(z) = \int_0^\infty \frac{\left[\sum_i f_i \delta(\epsilon_i - \epsilon) + g(\epsilon)\right] d\epsilon}{\epsilon^2 - z^2} \quad . \tag{1}$$

Equation (1) defines an analytic function in the cut z plane having simple poles at the discrete-excitation energies of the system ϵ_i and an imaginary discontinuity on the real axis beginning at the ionization threshold. The total photoabsorption cross section is related to the magnitude of the imaginary discontinuity of $\alpha(z)$ across the real energy axis by the expression[30]

$$\sigma(\omega) = \lim_{\epsilon \to 0} \frac{4\pi\omega}{c} \operatorname{Im}[\alpha(\omega + i\epsilon)] = \frac{2\pi^2}{c} g(\omega). \tag{2}$$

Although evaluation of Eqs. (1) and (2) apparently re-

quires prior knowledge of the discrete and continuum portions of the appropriate oscillator-strength profile, an alternative computational approach is provided by consideration of the cumulative oscillator-strength distribution

$$f(\epsilon) = \int_0^{\epsilon} \left[\sum f_i \delta(\epsilon_i - \epsilon') + g(\epsilon') \right] d\epsilon' = \int_0^{\epsilon} df(\epsilon'), \tag{3}$$

which is uniquely determined by its power moments[29]

$$S(-k) = \int_0^{\infty} \epsilon^{-k}\, df(\epsilon), \quad k = 0, 1, \ldots \quad . \tag{4}$$

Following the Stieltjes procedure, the cumulative oscillator strength [Eq. (3)] is approximated by an n-term histogram of the form[10]

$$f(\epsilon) \approx F^{(n)}(\epsilon) = \sum_{\epsilon_\alpha < \epsilon} f_\alpha, \quad \epsilon_\alpha \neq \epsilon, \tag{5}$$

where the n points and weights $\{\epsilon_\alpha, f_\alpha\}$, which are distinct from the correct discrete spectrum $\{\epsilon_i, f_i\}$ of Eq. (1), are obtained by solving the generalized quadrature problem associated with the specification of $2n$ values of the moments[13]

$$S(-k) = \sum_{\alpha=1}^{n} f_\alpha \epsilon_\alpha^{-k}, \quad k = 0, 1, \ldots, 2n-1. \tag{6}$$

If the $2n$ sequential moments employed in Eq. (6) are precisely those of Eq. (4) the n associated quadrature points and weights, which provide a *principal representation* of the moments, have particularly useful properties. Specifically, in this case the histogram of Eq. (5) rigorously bounds the correct distribution through the Tchebycheff inequalities[13]

$$F^{(n)}(\epsilon_\alpha - 0) < f(\epsilon_\alpha) < F^{(n)}(\epsilon_\alpha + 0), \tag{7}$$

and converges to $f(\epsilon)$ in the limit $n \to \infty$. When variationally determined or other approximate spectral moments are employed in Eq. (6), the bounds of Eq. (7) and the associated convergence properties are no longer rigorous and it is important to require that $n \ll N$.[10,11]

In order to obtain an approximation to the photoionization density $g(\epsilon)$ it is necessary to differentiate the cumulative histogram of Eq. (5) in some fashion. Considerable flexibility exists in this aspect of the moment-theory development, and various techniques have been employed.[9-11,14-19,31,32] The bounds of Eq. (7) suggest that convergent approximations to the continuum oscillator strength can be obtained at the successive points

$$\omega_\alpha = (1/2)(\epsilon_\alpha + \epsilon_{\alpha+1}) \tag{8a}$$

from the slopes of straight-line segments connecting adjacent Stieltjes values of the cumulative histogram $F^{(n)}(\epsilon)$ in the form of the so-called Stieltjes derivative,[10]

$$g(\omega_\alpha) = G^{(n)}(\omega_\alpha) = (\tfrac{1}{2})(f_\alpha + f_{\alpha+1})/(\epsilon_{\alpha+1} - \epsilon_\alpha). \tag{8b}$$

The discrete data points of Eqs. (8) are conveniently fit with appropriate analytic expressions, for which purpose simple polynomials in $1/\epsilon$ and rational fractions have proved useful.[10,32] Alternatively, analytic forms can be fit to the discrete cumulative values $F^{(n)}(\omega_\alpha)$ and differentiated to obtain a continuous convergent approximation to $g(\epsilon)$ in the photoionization region. Polynomials in $1/\epsilon$ and cubic natural spline functions, which provide a representation with continuous first and second derivatives, have proved useful in this connection.[10,16,19]

A continuous convergent approximation to the cumulative oscillator-strength distribution is obtained from the Tchebycheff development by preassigning the energy ϵ and solving the moment problem of Eq. (6) for its associated weight $f_0(n, \epsilon)$ and $n-1$ additional points and weights $\epsilon_\alpha(\alpha)$ and $f_\alpha(n, \epsilon)$, which depend parametrically on ϵ.[11] The discrete and continuum portions of the oscillator-strength profile are obtained from the Stieltjes values of the cumulative distribution in the form of the so-called Tchebycheff derivative[11]

$$G^{(n)}(\epsilon) = \frac{1}{2} \frac{df_0(n, \epsilon)}{d\epsilon} + \sum_\alpha \frac{df_\alpha(n, \epsilon)}{d\epsilon} \quad , \tag{9}$$

where the sum in Eq. (9) is over all weights for which $\epsilon_\alpha < \epsilon$. The analytic properties of Eq. (9) have been investigated in detail and its convergence in the limit $n \to \infty$ established.[11(c)] Moreover, previous applications indicate that Eq. (9) is computationally satisfactory, providing smooth convergent profiles in the photoionization region, and delta-functionlike structures at the appropriate discrete-transition frequencies.[11]

In the course of numerical applications it is convenient to work with the recurrence coefficients for the orthogonal polynomials of the associated generalized quadrature problem.[13] These coefficients $\{\alpha_n, \beta_n\}$ are recursively evaluated by means of a stable algorithm involving only variationally determined pseudospectra.[11(b)] When the orthogonal polynomials have been determined, the set of points and weights $\{\epsilon_\alpha, f_\alpha\}$ required in the Stieltjes–Tchebycheff analysis are obtained from their roots and the residues of related rational fractions.[10,11]

Although it is not possible in general to obtain an exact principal representation [Eq. (6)] for the oscillator-strength profile of an arbitrary many-electron system, experience indicates that finite Hilbert space calculations, which give N discrete energies and f values, can provide $2n$ accurate power moments for $n \ll N$.[10,11,14-19] This observation forms the basis for an attractive computational procedure in which pseudostate spectra obtained from normalizable basis functions provide the information required for a Stieltjes–Tchebycheff moment analysis, thus avoiding entirely the use of many-electron continuum molecular wavefunctions in photoionization calculations. Consequently, the effects of configuration interaction in atomic and molecular continua, and the continuum spectra of nonlocal and noncentral potentials, can be investigated in this way employing conventional bound-state computational technology.[12]

III. L^2 DISCRETIZATION OF THE MOLECULAR CONTINUUM

The total photoabsorption cross section of a many-electron system can be written as a sum of partial cross

sections for the various energetically open channels in the form

$$\sigma(\omega) = \sum_{\Gamma} \sigma_{\Gamma}(\omega), \tag{10}$$

where the individual partial cross sections are defined by

$$\sigma_{\Gamma}(\omega) = \frac{4\pi^2\omega}{3c} \left| \langle \Psi_{\Gamma}^{-} | \mu | \Psi_0 \rangle \right|^2 , \tag{11}$$

Ψ_0 is the initial wavefunction of the bound system, μ is the dipole vector, and Ψ_{Γ}^{-} is a molecular continuum function satisfying incoming boundary conditions which describes a free-electron incident on an ionic state labeled by Γ. Each channel function Ψ_{Γ}^{-} contains scattered-wave components which give the inelastic amplitudes for scattering out of state Γ into all other open ionic channels Γ'.

In finite basis-set calculations, the continuum channel functions are approximated at discrete-energy eigenvalues by associated eigenvectors which represent, apart from an overall normalization, some linear combination of open-channel solutions.[33] Formally, it is not necessary to specify these linear combinations in computing *total* photoionization cross sections, since a complete set of states can be constructed from linear combinations of the physical scattering states. Although the theorems from the theory of moments employed here are quite generally applicable, care must be exercised in applying the Stieltjes–Tchebycheff procedure when the excitation spectrum studied is a superposition of weakly interacting physically distinct components. Previous computational experience[34] indicates that structures associated with autoionizing states and the opening of new ionic continua at the various thresholds are poorly imaged in total cross-section calculations unless very large basis sets are employed and the effects of molecular symmetry are particularly favorable,[18] or unless appropriate projection techniques are introduced.[35]

A useful approximate solution of the coupled-channel problem which avoids the potentially superious results arising from weak interactions, but does not require an elaborate projection operator formalism, is obtained in the present development by separating out the various physically distinct low-lying ionic states of N_2^+, constructing wavefunctions for such states, and using these wavefunctions to define ionic molecular fields in which the active electron is allowed to move. Each molecular-ionic wavefunction defines an effective one-particle potential which, of course, reflects the nonspherical nature of the molecular core and also contains a nonlocal component. Dipole-allowed total molecular states are constructed by coupling a single-particle molecular orbital of the appropriate symmetry to make $^1\Sigma_u^+$ or $^1\Pi_u$ states, which are the only optically allowed states in homonuclear diatomic molecules that have $^1\Sigma_g^+$ initial states. Coupling between the different ionic channels is ignored, providing results equivalent to the use of static-exchange potentials for each ionic channel. The total photoabsorption cross section is obtained by summing the contributions from all such channels. If necessary, the importance of channel coupling can be assessed in the context of L^2 calculations by adopting an appropriate projection formalism and constructing appropriate quadrature approximations to the cross-channel integrals,[33,35] procedures which are beyond the scope of the present study.

Attention is restricted here to consideration of the three lowest ionic states of N_2^+—$X^2\Sigma_g^+$, $A^2\Pi_u$, and $B^2\Sigma_u^+$—which have vertical ionization potentials of 15.6, 16.7, and 18.8 eV, respectively,[26] and are expected to provide the major contribution for the formation of N_2^+ in photoionization.[25,27] There are seven possible allowed final states in this approximation which can connect to the ground $X^1\Sigma_g^+$ state of N_2, designated as

$$\begin{aligned}
&(1\sigma_g^2 1\sigma_u^2 2\sigma_g^2 2\sigma_u^2 1\pi_u^4 3\sigma_g\, k\sigma_u),\ ^1\Sigma_u^+\\
&(1\sigma_g^2 1\sigma_u^2 2\sigma_g^2 2\sigma_u^2 1\pi_u^4 3\sigma_g\, k\pi_u),\ ^1\Pi_u\\
&(1\sigma_g^2 1\sigma_u^2 2\sigma_g^2 2\sigma_u^2 1\pi_u^3 3\sigma_g^2\, k\sigma_g),\ ^1\Pi_u\\
&(1\sigma_g^2 1\sigma_u^2 2\sigma_g^2 2\sigma_u^2 1\pi_u^3 3\sigma_g^2\, k\pi_g),\ ^1\Sigma_u^+\\
&(1\sigma_g^2 1\sigma_u^2 2\sigma_g^2 2\sigma_u^2 1\pi_u^3 3\sigma_g^2\, k\delta_g),\ ^1\Pi_u\\
&(1\sigma_g^2 1\sigma_u^2 2\sigma_g^2 2\sigma_u 1\pi_u^4 3\sigma_g^2\, k\sigma_g),\ ^1\Sigma_u^+\\
&(1\sigma_g^2 1\sigma_u^2 2\sigma_g^2 2\sigma_u 1\pi_u^4 3\sigma_g^2\, k\pi_g),\ ^1\Pi_u\ .
\end{aligned} \tag{12}$$

In each of these seven cases, a set of N orbitals Φ_k, and hence N energies and oscillator strengths, is obtained from a single diagonalization of the appropriate one-particle Hamiltonian associated with the residual ion core. The equations to be solved can be written as

$$\langle \Phi_j | H^{\Gamma} | \Phi_k \rangle = \epsilon_k \delta_{jk} , \tag{13a}$$

$$H^{\Gamma} = T + V + \sum_i 2J_i - K_i + J_{\Gamma} + K_{\Gamma}, \tag{13b}$$

where T and V are the kinetic-energy and nuclear-framework potential-energy operators, J and K are the usual Coulomb and exchange operators (not including spin), the sum on i runs over all doubly occupied orbitals in the ion core, and Γ refers to the singly occupied open-shell orbital of the ion. Equations (13) indicate that the $\{\Phi_k\}$ are equivalent to the virtual orbitals of the V_{N-1} potential,[36,37] which are frequently used in bound-state molecular applications.[38] Such functions, which can be designated as *improved virtual orbitals*,[38] exhibit the correct molecular Rydberg structure, are closely related to functions obtained in the random-phase approximation,[39] and should provide a reliable description of unbound molecular states, as well.

Since Eqs. (13) entail computations with SCF Hamiltonians, the present approach allows construction of the discrete pseudospectra required for the Stieltjes–Tchebycheff moment analysis from diagonalization of relatively small matrices. Furthermore, there is no reason to use the same set of basis functions to expand both the occupied core orbitals and the virtual orbitals Φ_k. In solving for the self-consistent occupied orbitals, a modest number of valencelike basis functions with optimized orbital exponents is employed. However, since a fairly rich spectrum is required to obtain the first few members of the appropriate Rydberg series and to carry out the moment analysis, the Hamiltonian of Eq.

(13b) is diagonalized over a much larger set of basis functions. Since this augmented set is considerably larger than the original set employed in the SCF calculations, some care is taken to see that only the necessary number of two-electron integrals is evaluated. If M functions are used in solving the SCF equations, and N functions are used to expand the virtual orbitals ($N \gg M$), the number of two-electron integrals needed goes as $N^2 \times M^2$. By contrast, a CI calculation in this basis requires the full number of two-electron integrals ($\sim N^4$) and a transformation of these which is an N^5 operation.[40]

In concluding this section, it is perhaps appropriate to note again that results obtained from Eqs. (13) and the Stieltjes–Tchebycheff technique for the particular case of photoionization in a homonuclear diatomic are equivalent to the so-called static-exchange approximation. In the case of heteronuclear diatomic molecules, additional complications arise in this approximation due to the presence of occupied and dipole-excited orbitals of the same symmetry type.[41]

IV. COMPUTATIONAL ASPECTS

An SCF wavefunction for the ground $^1\Sigma_g^+$ state of N_2 at $R_e = 2.068$ a.u. is obtained in the basis set of [4s, 3p] +1d ($\alpha = 0.8$) contracted Gaussian functions given by Dunning,[42] providing a total energy of -108.964 a.u. compared to the accepted Hartree–Fock limit of -108.993 a.u.[43] Approximate N_2^+ wavefunctions are formed by removing one of the three occupied valence orbitals ($3\sigma_g$, $1\pi_u$, or $2\sigma_u$), and the static-exchange Hamiltonians for these states are diagonalized over a large set of symmetry-adapted basis orbitals. These basis sets are formed by augmenting the SCF basis with additional appropriate functions. For the $3\sigma_g \rightarrow n\sigma_u$ transitions four additonal s-type and four p_z-type Gaussians are placed on the nitrogens, and up to fifteen additional p_z-type functions are placed at the center of the molecule. Four independent sets of calculations are performed in this case, and it is found that the final cross sections are relatively insensitive to the choice of orbital exponents, varying by less than 10% from one another over an energy range from threshold to 50 eV above the IP. The results reported here are obtained using ten p_z functions at the midpoint of the molecule with exponents chosen to span the range from 0.2 to 0.0003 in a geometric series. Similar choices are made in carrying out the remaining calculations, placing four additional functions of the appropriate symmetry type on each nitrogen atom (s, p_x, p_z, d_{xz}, or d_{xy}), and 15 at the midpoint. The basis sets employed are found to provide adequate representations of the first five or so discrete Rydberg states, and to provide pseudospectra above the ionization limits which are sufficiently dense for a successful moment analysis.

The Stieltjes–Tchebycheff moment analysis is found to provide stable results using up to 20 power moments calculated from the static-exchange pseudospectra. Higher-order computations reveal the underlying discrete nature of the pseudospectra, suggesting that approximately ten principal pseudostates[10b] are correctly described by the basis sets employed in each case. In order to obtain fully convergent Tchebycheff profiles it is desirable to use a larger number of moments, since calculations carried out using too few moments can give cross sections which display small unphysical oscillations as a function of energy.

High-order moments are obtained from the previously described extrapolation technique employing asymptotic values which depend only on the ionization threshold in the form[11b,44]

$$\alpha^\infty = 1/(2\epsilon_t), \tag{14a}$$

$$\beta^\infty = 1/(4\epsilon_t)^2. \tag{14b}$$

Although the total photoionization cross section in N_2 is structured, the individual channel contributions are relatively simple profiles. Consequently, the calculated recurrence coefficients are reliably extended to the asymptotic values of Eqs. (14) using previously described analytical forms.[11b] This procedure is found to yield highly satisfactory results in the present case.

Since merely deleting one orbital from the SCF wavefunction of N_2 does not allow for proper relaxation of the remaining ionic core, it is important to investigate contributions from this effect by performing separate open-shell SCF calculations on each ionic state. This considerably complicates the evaluation of dipole matrix elements, since the orbitals describing the determinantal wavefunctions of the initial and final states are no longer orthogonal. Nevertheless, the possible importance of relaxation effects are investigated in calculations on the $3\sigma_g \rightarrow n\sigma_u$ transitions using a configuration–interaction technique. A set of final-state wavefunctions is obtained by employing both N_2 and N_2^+ SCF orbitals and including all single excitations of the type $3\sigma_g \rightarrow n\sigma_u$. Similarly, a correlated ground-state wavefunction for N_2 is obtained from the same calculations. The resulting photoabsorption cross section for the $3\sigma_g \rightarrow n\sigma_u$ channel is found to differ insignificantly from the values obtained in the static-exchange approximation. A similar insensitivity to relaxation effects in the other photoionization channel calculations reported here is expected, although such effects can be important in core–electron ionization cross sections, and in determining the properties of discrete low-lying valencelike states.[19] These effects are discussed somewhat further below in specific cases.

V. MOLECULAR NITROGEN RESULTS

Solutions of the static-exchange equations [Eqs. (13)] provide seven distinct sets of eigenvectors and associated energies which correspond to the ionization potentials of the virtual orbitals. In order to obtain excitation energies out of the ground state, which are required in computing oscillator strengths, the IP's of the ground and excited states are combined according to the expression

$$\omega_{0k} = IP_0 + \epsilon_k \ . \tag{15}$$

The computed excitation energies and oscillator strengths obtained using Eq. (15) and vertical ionization potentials of 15.6, 16.7, and 18.8 eV for the $X^2\Sigma_g^+$, $A^2\Pi_u$, and $B^2\Sigma_u^+$ states of N_2^+, respectively,[26] are given

TABLE I. Pseudospectrum of transition frequencies and oscillator strengths for the process $\hbar\omega + N_2(X\,^1\Sigma_g^+) \rightarrow N_2^+(X\,^2\Sigma_g^+) + e^-$ calculated in the static-exchange approximation.[a]

$(3\sigma_g)\,^1\Sigma_g^+ \rightarrow (n\sigma_u)\,^1\Sigma_u^+$		$(3\sigma_g)\,^1\Sigma_g^+ \rightarrow (n\pi_u)\,^1\Pi_u$	
ω_{on}	f_{on}[b]	ω_{on}	f_{on}[b]
0.483 506	0.059 153	0.479 339	0.068 082
0.530 109	0.019 033	0.528 293	0.020 300
0.547 783	0.008 583	0.546 885	0.008 778
0.556 499	0.004 640	0.555 989	0.004 653
0.561 623	0.003 149	0.561 230	0.003 123
0.565 012	0.005 076	0.564 477	0.003 258
0.590 432	0.037 416	0.566 690	0.000 707
0.658 200	0.002 628	0.586 881	0.029 246
0.685 623	0.142 612	0.666 763	0.046 265
0.903 108	0.010 275	0.728 270	0.114 375
0.918 179	0.356 214	0.875 084	0.025 564
1.186 304	0.358 020	1.155 049	0.430 751
1.373 871	0.004 047	1.337 526	0.013 758
1.640 533	0.020 639	1.923 903	0.468 831
2.009 566	0.007 749	2.201 600	0.014 173
2.508 185	0.029 042	3.444 786	0.160 269
3.316 339	0.004 096	3.863 528	0.003 001
4.157 971	0.039 324	4.358 399	0.005 545
4.462 802	0.013 868	6.727 269	0.012 695
6.741 453	0.000 761	7.170 216	0.010 616
8.846 050	0.020 611	14.751 288	0.000 729
37.892 974	0.003 593	19.219 302	0.005 989

[a]All quantities are in Hartree atomic units.
[b]f numbers appropriate for the total line strengths, including all degenerate components.

in Tables I–III. By employing the experimentally determined ionization potentials in Eq. (15) the various calculated Rydberg series are made to converge at the appropriate positions. Moreover, the well-known error in the ordering of Koopmans ionization potentials in molecular nitrogen is thereby circumvented.[12]

The lowest members of each series shown in Tables I–III, corresponding to virtual orbitals with negative energies, provide approximations to the appropriate Rydberg states. A comparison of the present results with experimental estimates and previous theoretical calculations for the Rydberg series converging on the ground $X^2\Sigma_g^+$ state of N_2^+ is given in Table IV. The experimental assignments and transition frequencies shown are taken from the recent detailed review of Lofthus and Krupenie,[23] and the references cited therein. The values shown for the experimental excitations in each series correspond to band maxima,[20] which are expected to be good approximations to the associated vertical electronic excitation energies in these cases. Evidently, the present static-exchange or IVO calculations are in good accord with the experimental transition frequencies, and with the previously reported theoretical values for these series.[8] The most significant discrepancies occur in the cases of the $3\sigma_g \rightarrow 2\pi_u$ transition, corresponding to excitation into the $c_3\,^1\Pi_u$ state,[23] and the $3\sigma_g \rightarrow 3\sigma_u$ excitation, corresponding to transition into the $c_4'\,^1\Sigma_u^+$ state.[23] Since the $2\pi_u$ orbital, which correlates with the $3p\pi$ united-atom limit,[45] is the lowest-lying Rydberg orbital in the $(n\pi_u)\,^1\Pi_u$ Worley–Jenkins series, and the $3\sigma_u$ is the lowest in the $(n\sigma_u)\,^1\Sigma_u^+$ series, correlating with the $4p\sigma$ united-atom orbital,[45] their positions and forms are expected to be more sensitive to the core-relaxation effects neglected in the present calculations than are the higher-lying Rydberg states. Although the available absorption data does not warrent a detailed comparison with theory, it is appropriate to note that the observed integrated band intensities[20] are in general accord with the calculated f numbers for the $3\sigma_g \rightarrow n\sigma_u$ and $n\pi_u$ series shown in Table I. Of course, the band intensities for the Rydberg series are perturbed by interactions with the $b'\,^1\Sigma_u^+$ and $b\,^1\Pi_u$ valence states,[22b] which are neglected in the present calculations. Tables I and IV indicate that the transition frequencies and oscillator strengths in the $(n\sigma_u)\,^1\Sigma_u^+$ and $(n\pi_u)\,^1\Pi_u$ series are highly similar. Moreover, since these correspond to $3\sigma_g$ transitions into $np\sigma$ and $np\pi$ series,[45] the positions and strengths approach the same limits for large n. On this basis it is possible to anticipate that the associated photoionization continua will be equal at the ionization threshold.

In Table V the theoretically determined discrete series for excitations of the $1\pi_u$ orbital are compared with two Rydberg series identified in this general spectral interval,[23] and with previously reported theoretical calculations.[8] Evidently, the theoretically determined $1\pi_u \rightarrow n\sigma_g$ positions are in general mutual accord and in good agreement with Worley's third Rydberg series for $^1\Pi_u$ excitation. Moreover, the calculated f numbers (Table II) are in general agreement with the observed band intensities.[20] The second member of this series is

TABLE II. Pseudospectrum of transition frequencies and oscillator strengths for the process $\hbar\omega + N_2(X\,^1\Sigma_g^+) \rightarrow N_2^+(A\,^2\Pi_u) + e^-$ calculation in the static-exchange approximation.[a]

$(1\pi_u)\,^1\Sigma_g^+ \rightarrow (n\sigma_g)\,^1\Pi_u$		$(1\pi_u)\,^1\Sigma_g^+ \rightarrow (n\pi_g)\,^1\Sigma_u^+$		$(1\pi_u)\,^1\Sigma_g^+ \rightarrow (n\delta_g)\,^1\Pi_u$	
ω_{on}	f_{on}[b]	ω_{on}	f_{on}[b]	ω_{on}	f_{on}[b]
0.490 629	0.148 961	0.525 631	1.265 385	0.560 133	0.027 444
0.560 261	0.584 099	0.570 296	0.154 122	0.585 106	0.014 946
0.584 908	0.030 204	0.589 539	0.048 428	0.596 648	0.008 337
0.596 482	0.018 090	0.598 970	0.022 021	0.602 888	0.005 191
0.602 862	0.012 393	0.604 311	0.013 533	0.606 607	0.003 348
0.606 688	0.008 369	0.614 879	0.053 050	0.612 920	0.014 139
0.609 746	0.002 021	0.655 127	0.091 268	0.636 771	0.048 097
0.617 945	0.047 420	0.754 938	0.060 933	0.696 603	0.131 452
0.643 019	0.000 327	0.871 024	0.000 835	0.823 713	0.269 111
0.714 600	0.130 596	0.962 727	0.010 279	0.945 673	0.047 163
0.868 720	0.122 421	1.181 370	0.004 609	1.086 571	0.339 108
0.957 457	0.096 735	1.329 090	0.001 194	1.581 340	0.298 262
1.172 601	0.013 279	1.534 385	0.015 753	1.907 558	0.025 065
1.394 285	0.075 570	1.945 324	0.005 665	2.585 666	0.149 239
1.619 557	0.054 085	2.360 869	0.023 737	4.209 551	0.068 221
2.026 275	0.043 478	2.921 183	0.016 819	4.683 175	0.006 677
2.587 475	0.005 178	3.120 663	0.000 044	8.784 673	0.001 283
2.925 207	0.066 182	3.755 941	0.023 056	10.545 989	0.018 107
3.572 649	0.019 723	4.718 761	0.014 538	18.173 712	0.000 003
4.399 310	0.000 611	5.573 318	0.011 200		
5.422 639	0.008 404	6.310 620	0.012 262		
5.872 230	0.001 219	7.814 579	0.024 431		
6.444 865	0.000 369	9.443 532	0.005 931		
7.714 664	0.000 001	10.976 257	0.003 127		
12.000 144	0.003 458	13.413 407	0.003 555		
13.398 564	0.001 838	21.070 373	0.000 235		
20.336 501	0.000 032	24.202 181	0.000 058		
46.515 907	0.000 207				

[a]All quantities are in Hartree atomic units.
[b]f-numbers appropriate for the total line strengths, including all degenerate components.

TABLE III. Pseudospectrum of transition frequencies and oscillator strengths for the process $\hbar\omega + N_2(X\,^1\Sigma_g^+) \rightarrow N_2^+(B\,^2\Sigma_u^+) + e^-$ calculated in the static-exchange approximation.[a]

$(2\sigma_u)\,^1\Sigma_g^+ \rightarrow (n\sigma_g)\,^1\Sigma_u^+$		$(2\sigma_u)\,^1\Sigma_g^+ \rightarrow (n\pi_g)\,^1\Pi_u$	
ω_{on}	f_{on}[b]	ω_{on}	f_{on}[b]
0.572 783	0.000 326	0.513 339	0.747 393
0.636 434	0.000 684	0.639 035	0.003 595
0.659 418	0.001 932	0.661 487	0.000 975
0.670 364	0.002 755	0.671 905	0.000 395
0.676 477	0.003 282	0.677 619	0.000 204
0.680 177	0.003 124	0.686 334	0.000 646
0.683 225	0.001 025	0.722 447	0.000 545
0.689 229	0.026 916	0.817 844	0.001 772
0.716 640	0.019 058	0.940 026	0.001 849
0.797 435	0.000 953	1.022 943	0.035 721
0.943 087	0.131 068	1.257 855	0.000 895
1.047 469	0.000 948	1.387 481	0.122 292
1.243 181	0.091 402	1.605 579	0.0
1.479 284	0.074 858	2.006 873	0.152 480
1.715 373	0.008 555	2.444 992	0.000 495
2.106 340	0.112 648	2.986 435	0.115 766
2.686 262	0.001 882	3.194 038	0.027 137
3.027 274	0.003 046	3.845 359	0.000 119
3.660 031	0.054 100	4.799 141	0.112 974
4.503 616	0.008 292	5.668 205	0.004 302
5.517 028	0.010 711	6.395 614	0.011 701
5.986 221	0.000 542	7.916 754	0.047 268
6.558 617	0.013 399	9.553 755	0.025 247
7.833 548	0.038 966	11.089 815	0.012 413
12.122 425	0.001 920	13.573 466	0.001 213
13.588 421	0.000 493	21.191 517	0.041 984
20.444 404	0.028 750	24.405 103	0.001 893
46.663 674	0.000 048		

[a]All quantities are in Hartree atomic units.

[b]f-numbers appropriate for the total line strengths, including all degenerate components.

is evidently quite intense, corresponding to transition into a relatively compact $5\sigma_g$ orbital, which correlates with a low-lying $3d\sigma$ orbital in the united-atom limit. Note that the previous calculations[8] give both $ns\sigma$ and $nd\sigma$ excitation series, whereas the present results employing only s-type diffuse functions for $n\sigma_g$ excitations provide a single Rydberg series in this case. The recently assigned $(nd\sigma_g)\,^1\Pi_u$ series[22b] (not shown in Table V) is not in very good accord with the previously reported calculations.[8] The theoretical $1\pi_u \rightarrow (n\delta_g)\,^1\Pi_u$ series is somewhat weak (Table II), and apparently has not been identified as yet in photoabsorption. Since the calculated $(n\delta_g)\,^1\Pi_u$ energies are essentially identical with the second and higher members of the $(n\sigma_g)\,^1\Pi_u$ series, it is plausible to suggest that the two, in fact, interact strongly and together account for the observed $^1\Pi_u$ series. The calculated $1\pi_u \rightarrow n\pi_g$ excitations are in good mutual accord and in general agreement with the positions and strengths of the Ogawa–Tanaka series for $^3\Pi_u$ excitation, although the overall symmetry is, of course, incorrect. Note that the theoretically determined $1\pi_u \rightarrow (1\pi_g)\,^1\Sigma_u^+$ state is not properly regarded as a member of the Rydberg series, but rather provides an approximation to the $b'\,^1\Sigma_u^+$ valence state[23]; that is the $1\pi_u \rightarrow 1\pi_g$ excitation refers to the familiar very intense $\pi \rightarrow \pi^*$ transition.[46]

In Table VI, the calculated $2\sigma_u \rightarrow (n\sigma_g)\,^1\Sigma_u^+$ and $2\sigma_u \rightarrow (n\pi_g)\,^1\Pi_u$ excitations are compared with the experimentally determined Hopfield strong absorption and window-emission series,[23] employing the conventional assignments $2\sigma_u \rightarrow (nd\sigma)\,^1\Sigma_u^+$ and $2\sigma_u \rightarrow (ns\sigma)\,^1\Sigma_u^+$, respectively, for the latter.[45] Note that the first members of each of the theoretically determined excitations should be regarded as extraneous, and correspond to approximations to the $b'\,^1\Sigma_u^+$ and $b\,^1\Pi_u$ valence states.[23] Evidently,

TABLE IV. Rydberg transition energies in N_2 converging on the ground $X\,^2\Sigma_g^+$ state of N_2^+.[a]

	$(3\sigma_g)\,^1\Sigma_g^+ \rightarrow (n\sigma_u)\,^1\Sigma_u^+$			$(3\sigma_g)\,^1\Sigma_g^+ \rightarrow (n\pi_u)\,^1\Pi_u$	
Present results[b]	Experimental values[c]	Previous calculations[d]	Present results[b]	Experimental values[c]	Previous calculations[d]
13.15	13.18	12.73	13.03	13.20	13.72
14.41	14.35	14.27	14.36	14.32	14.60
14.89	14.86	14.82	14.87	14.83	14.97
15.13	15.10	15.07	15.12	15.09	15.16
15.27	15.23	15.22	15.26	15.22	15.27
15.36	15.32	15.31	15.35	15.31	15.35
			15.40	15.32	15.39

[a]All values in electron volts.

[b]Values taken from Table I.

[c]R. E. Worley and F. A. Jenkins, Phys. Rev. **54**, 305 (1938); M. Ogawa and Y. Tanaka, Can. J. Phys. **40**, 1593 (1962); P. K. Carroll and C. P. Collins, Can. J. Phys. **47**, 563 (1969); P. K. Caroll and K. Yoshino, J. Chem. Phys. **47**, 3073 (1967); J. Phys. B **5**, 1614 (1972). The members of each series correspond to estimated band maxima (Ref. 20). Recent synchrotron radiation measurements [Ref. 22(b)] suggest the maximum for the $3\sigma_g \rightarrow 3\sigma_u$ excitation should occur at 12.93 eV, rather than 13.18 eV.

[d]C. Duzy and R. S. Berry, J. Chem. Phys. **64**, 2421 (1976); see also, H. Lefebvre-Brion, and C. Moser, J. Chem. Phys. **43**, 1394 (1965); A. B. F. Duncan and A. Damiani, J. Chem. Phys. **45**, 1245 (1966).

TABLE V. Rydberg transition energies in N_2 converging on the $A\,^2\Pi_u$ state of N_2^+.[a]

Theoretical results[b]			Experimental values[c]	
$(1\pi_u)\,^1\Sigma_g^+ \rightarrow (n\sigma_g)\,^1\Pi_u$	$(1\pi_u)\,^1\Sigma_g^+ \rightarrow (n\pi_g)\,^1\Sigma_u^+$	$(1\pi_u)\,^1\Sigma_g^+ \rightarrow (n\delta_g)\,^1\Pi_u$	$^1\Pi_u$ series	$^3\Pi_u$ series
13.34 (12.58, 12.44)	14.29 (13.26)	15.23 (15.75)	13.34	...
15.23 (15.15, 15.37)	15.51 (15.49)	15.91 (15.84)	15.36	15.47
15.90 (15.85, 15.94)	16.03 (15.99)	16.22 (16.18)	16.06	15.97
16.22 (16.16, 16.21)	16.29 (16.26)	16.39 (16.35)	16.33	16.33
16.39 (16.33, 16.36)	16.43 (16.40)	16.49 (16.44)	16.54	16.50
16.50 (16.43, 16.45)	16.72 (16.48)	16.67 (16.52)	16.64	16.64

[a]All values in electron volts.

[b]Values taken from Table II. Those in parenthesis are from C. Duzy and R. S. Berry, J. Chem. Phys. 64, 2421 (1976). The entries in parenthesis in the first column refer to the $ns\sigma$ and $nd\sigma$ series, respectively. See also, H. Lefebvre-Brion and C. Moser, J. Chem. Phys. 43, 1394 (1965).

[c]The $^1\Pi_u$ states refer to Worley's third series [R. E. Worley, Phys. Rev. 89, 863 (1953)], and the $^3\Pi_u$ states to the Ogawa and Tanaka series [M. Ogawa and Y. Tanaka, Can. J. Phys. 40, 1593 (1962)]. Transition frequencies shown correspond to vertical energies estimated from band maxima [see Refs. 20–23]. Recent synchrotron radiation studies [Ref. 22(b)] assign an $(nd\sigma)\,^1\Pi_u$ series in this region, in accordance with the analysis of E. Lindholm, Ark. Fys. 40, 111 (1969).

the calculated $2\sigma_u \rightarrow n\sigma_g$ series is not rich enough to account for both $nd\sigma$ and $ns\sigma$ excitations, although the theoretical positions in this case are in good accord with the observed $ns\sigma$ series. Examination of the orbital compositions of the calculated $n\sigma_g$ series indicates the presence of alternating $s\sigma$ and $d\sigma$ character. However, the diffuse d-type functions employed in the present calculations are insufficient to account fully for the $nd\sigma$ series. Moreover, the theoretical f numbers for the $2\sigma_u \rightarrow n\sigma_g$ series (Table III) are increasing with n, and it is not clear if this pattern is in accord with the window-emission line shapes.[22(b)] The $2\sigma_u \rightarrow (n\pi_g)\,^1\Pi_u$ series is evidently only in general accord with the $2\sigma_u \rightarrow nd\sigma$ strong absorption series positions, and the theoretically determined f numbers (Table III) are too small to account for the observed line strengths.[22(b)] We can conclude that the $2\sigma_u \rightarrow (n\pi_g)\,^1\Pi_u$ series is most likely too weak to be observed at present, and that autoionization lineshape calculations will be required to account quantitatively for the photoabsorption cross section in this spectral interval. In spite of the inability of the presently employed basis to account in detail for the closely spaced $nd\sigma$ and $ns\sigma$ series, we can nevertheless anticipate that the associated pseudospectra are sufficiently dense in this channel to give good results in the photoionization continuum.

The continuum pseudostates shown in Tables I–III are sufficiently dense to provide reliable Stieltjes–Tchebycheff profiles for excitation energies up to approximately 50 eV above threshold in each case, as will be clear from the subsequent comparisons given below. Note in this connection that the variational pseudospectra are irregular and do not yield reliable photoionization densities directly without performing a moment analysis. This is apparently a consequence of the nonlocal nature of the Fock potential. The individual components of the vertical electronic photoionization cross sections shown in Figs. 1–3, obtained from the recurrence coefficient extension procedure using Eqs. (14), are evidently in good accord with the selected values of eighth- through tenth-order Stieltjes results also shown and, consequently, provide a correct interpolation of the latter values.

TABLE VI. Rydberg transition energies in N_2 converging on the $B\,^2\Sigma_u^+$ state of N_2^+.[a]

Theoretical results[b]		Experimental values[c]	
$(2\sigma_u)\,^1\Sigma_g^+ \rightarrow (n\sigma_g)\,^1\Sigma_u^+$	$(2\sigma_u)\,^1\Sigma_g^+ \rightarrow (n\pi_g)\,^1\Pi_u$	$(2\sigma_u)\,^1\Sigma_g^+ \rightarrow (nd\sigma)\,^1\Sigma_u^+$	$(2\sigma_u)\,^1\Sigma_g^+ \rightarrow (ns\sigma)\,^1\Sigma_u^+$
15.57 (15.6)	13.96	...	...
17.30 (17.1)	17.38	17.13	17.32
17.93 (17.4)	17.99	17.83	17.95
18.23	18.27	18.16	18.22
18.39	18.42	18.34	18.38
18.49	18.66	18.45	18.49

[a]All values in electron volts.

[b]Values taken from Table III, except for those shown in parenthesis, which are from H. Lefebvre-Brion and C. Moser, J. Chem. Phys. 43, 1394 (1965).

[c]The second through sixth members of the $2\sigma_u \rightarrow nd\sigma$ series refer to the Hopfield strong absorption series [J. J. Hopfield, Phys. Rev. 35, 1133 (1930); 36, 789 (1030)], whereas the second through sixth members of the $2\sigma_u \rightarrow ns\sigma$ series refer to the emission or window resonance series [M. Ogawa and Y. Tanaka, Can. J. Phys. 40, 1593 (1962)]. The orbital assignments are originally due to Mulliken [R. S. Mulliken, Phys. Rev. 46, 144 (1934)].

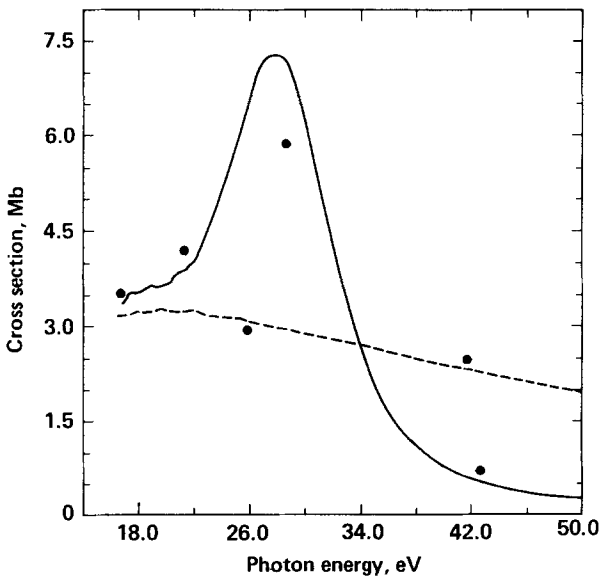

FIG. 1. Vertical electronic photoionization cross sections in N_2 for processes leading to production of $N_2^+(X\,^2\Sigma_g^+)$ obtained from the Stieltjes–Tchebycheff approach in the static-exchange approximation; solid line (—), $3\sigma_g \rightarrow k\sigma_u$ transitions; dashed line (----), $3\sigma_g \rightarrow k\pi_u$ transitions. Photon energy is in electron volts, and cross sections are in megabarns (1 Mb = 10^{-18} cm^2). The solid circles refer to selected eighth- to tenth-order Stieltjes values.

In accordance with the observation made above, the two photoionization continua for the $X^2\Sigma_u^+$ channel shown in Fig. 1 are evidently equal at threshold. The broad shape resonance with a maximum at ~28 eV in the $3\sigma_g \rightarrow k\sigma_u$ contribution to the $N_2(X\,^1\Sigma_g^+) + h\nu \rightarrow N_2^+(X\,^2\Sigma_g^+) + e^-$ photoionization channel can be attributed to the presence of valencelike σ_u pseudo-orbitals in the photoionization spectrum. According to the stabilization phenomenon,[33] an L^2 basis set will simulate the presence of resonance structures in scattering continua. Indeed, examination of the basis set compositions of the appropriate pseudo-orbitals (Table I) in this case reveals the influence of compact $2p$ atomic orbitals, accounting for the high intensity in the $3\sigma_g \rightarrow k\sigma_u$ channel in accordance with Mulliken's early analysis of transitions involving σ^* orbitals.[46] Of course, the position and detailed nature of the resonance is a quantitative question, which is settled in the present case by obtaining L^2 solutions in the nonlocal Fock potential of correct molecular symmetry. It is, perhaps, of interest to note in this connection that Mulliken has recently suggested the $3\sigma_g \rightarrow (3\sigma_u)\,^1\Sigma_u^+$ or V_σ state in N_2 will appear in the photoionization continuum due to configuration mixing with the $1\pi_u \rightarrow (1\pi_g)\,^1\Sigma_u^+$ or V_Π state.[47] Recent X_α studies[7(b)] attribute the large cross section in this case to an f-wave resonance in a body-centered partial-wave expansion. Examination of the resonance σ_u orbitals in a body-centered coordinate system reveals the presence of large p- and f-wave components, although the latter dominates at large radial distances. The f-wave resonance description is further clarified by noting that the pseudo σ_u orbitals can correlate with Rydberg $4f\sigma$ atomic orbitals in the united-atom limit, and are partially Rydbergized at the equilibrium internuclear separation.[48] That is, the σ_u pseudocontinuum orbital is valencelike in size but of high f-wave character at the equilibrium separation. Similar remarks have been made previously in connection with the $1\sigma_g \rightarrow k\sigma_u$ resonance in the N_2 K-shell photoionization cross section.[7(a),19]

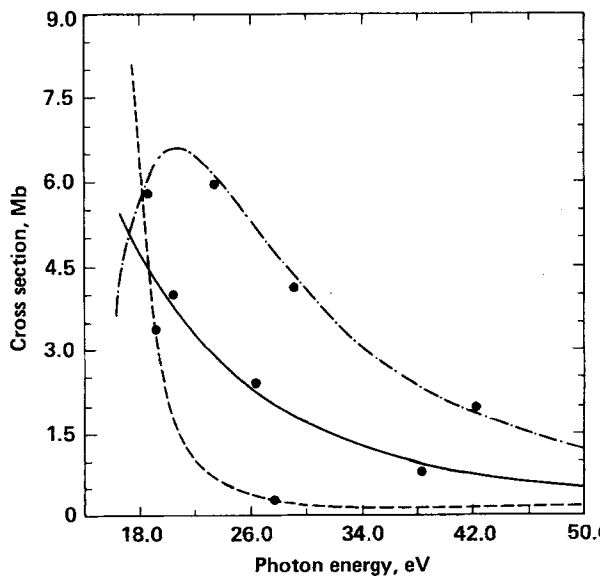

FIG. 2. As in Fig. 1, for the production of $N_2^+(A\,^2\Pi_u)$; solid line(—), $1\pi_u \rightarrow k\sigma_g$ transitions; dashed line (----), $1\pi_u \rightarrow k\pi_g$ transitions; dashed–dot line (– · – ·), $1\pi_u \rightarrow k\delta_g$ transitions.

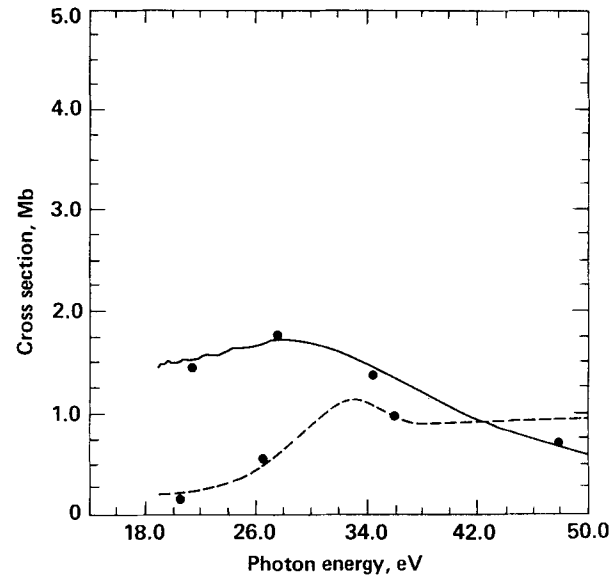

FIG. 3. As in Fig. 1, for the production of $N_2^+(B\,^2\Sigma_u^+)$; solid line (—), $2\sigma_u \rightarrow k\sigma_g$ transitions; dashed line (----), $2\sigma_u \rightarrow k\pi_g$ transitions.

In contrast to the $3\sigma_g \rightarrow k\sigma_u$ contribution, the $3\sigma_g \rightarrow k\pi_u$ photoionization cross section shown in Fig. 1 is monotonically decreasing in excitation energy. Although it is possible, in principle, for this channel to also exhibit resonancelike structures, it is highly unlikely that the Fock potential will support a valencelike π_u pseudo-orbital, in addition to the occupied valence $1\pi_u$. This is ultimately a quantitative question, however. Note that the f sum rule insures that the $3\sigma_g \rightarrow k\pi_u$ contribution

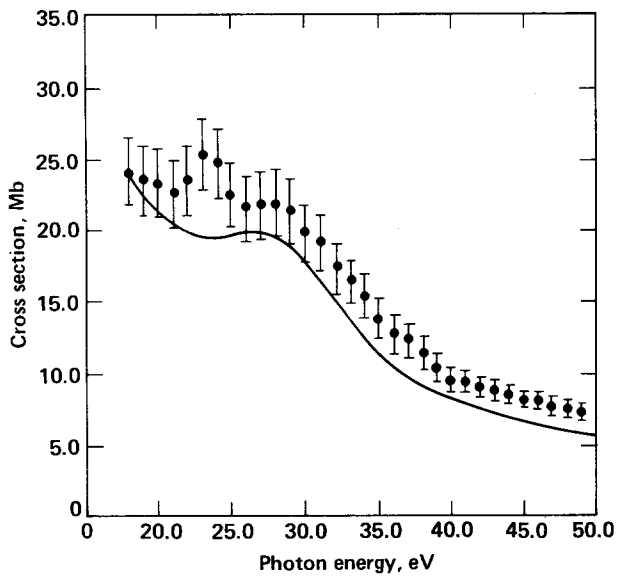

FIG. 4. Total photoionization cross section in N_2 for the production of N_2^+ ions; solid line (—), Stieltjes–Tchebycheff results in the static-exchange approximation obtained from Eq. (10) and Figs. 1–3; data points (●), electron-ion coincidence measurements of van der Wiel, *et al.* (Ref. 25). The ±10% error bars indicated are suggested nominal values and do not correspond to the combined random and systematic errors in the measurements.

will dominate this photoionization channel at high energy, since so much intensity is concentrated under the shape resonance in the $3\sigma_g \rightarrow k\sigma_u$ component.

Referring now to Fig. 2, the $1\pi_u \rightarrow k\pi_g$ contribution to this channel is evidently a rapidly decreasing function of excitation energy. This behavior is a consequence of the very intense $1\pi_u \rightarrow 1\pi_g(\pi \rightarrow \pi^*)$ discrete transition in this channel (Table II), which accounts for much of the f sum rule in this case. Similarly, the strong discrete transitions (Table II) in the $1\pi_u \rightarrow k\sigma_g$ channel insure that the associated continuum profile is also relatively rapidly decreasing with excitation energy. By contrast, there is an apparent resonancelike structure in the $1\pi_u \rightarrow k\delta_g$ channel, which can be attributed to relatively compact resonance orbitals which can correlate with $3d\delta$ orbitals in the united-atom limit. The lack or presence of resonancelike structures is ultimately a quantitative question, of course, although it is highly unlikely that the Fock potential will support compact π_g and σ_g orbitals in addition to the $1\pi_g(\pi^*)$ and $4\sigma_g$, $5\sigma_g$ discrete orbitals. In contrast, the δ_g spectrum evidently contains compact $3d\delta$ pseudo-orbitals in the continuum, but weak discrete components (Table II).

Referring now to Fig. 3, the two contributions to the photoionization channel for the removal of a $2\sigma_u$ electron are evidently small and relatively slowly varying functions of energy in this case. Because of the very intense $2\sigma_u \rightarrow 1\pi_g$ $(n \rightarrow \pi^*)$ discrete transition (Table III), the associated continuum is quite small at threshold, but comparable to the $2\sigma_u \rightarrow k\sigma_g$ contribution at higher excitation energies. Somewhat similar structure is observed in the K shell $1\sigma_u \rightarrow k\pi_g$ and $k\sigma_g$ photoionization cross sections.[7(a),19]

In order to construct photoionization cross sections from the vertical electronic profiles of Figs. 1–3, it is necessary to incorporate the appropriate Franck–Condon and Hönl–London factors for the three electronic transitions considered.[49] The situation is considerably simplified, however, by noting that the potential curves for the $X^2\Sigma_g^+$, $A^2\Pi_u$, and $B^2\Sigma_u^+$ states in N_2^+ are deep (~9, 8, and 6 eV binding energies, respectively) and approximately centered at the $X^1\Sigma_g^+ N_2$ equilibrium internuclear distance.[50] Consequently, the Franck–Condon regions for photoionization into these states do not extend far above the 0–0 thresholds, and vanish in the vibrational continuum.[51] Therefore, an excellent vibrational- and rotational-averaged approximation to the photoionization cross section in N_2 for the production of N_2^+ ions only is obtained from Eq. (10) by adding the partial vertical electronic cross sections of Figs. 1–3.[49]

In Fig. 4 is shown the photoionization cross section for the production of N_2^+ ions only obtained from Eq. (10) and Figs. 1–3, and from the recent electron–ion coincidence measurements of van der Wiel *et al.*[25] The theoretical predictions are evidently in excellent accord with the experimental values, except at approximately 23 eV, where a structure in the latter is absent in the former. This feature is discussed further below. A detailed comparison of results in the immediate vicinity of threshold is avoided, since the effects of vibrational structure are neglected in the present calculations. It is particularly noteworthy that the calculations are uniformly below the measured values, and that the inflection in the experimental data at ~27 eV, also discussed below, is accurately predicted by theory. Note in this connection that the ±10% experimental error bars indicated are suggested nominal values, and do not represent the combined absolute random and systematic errors of the measurements. An energy resolution of approximately 0.5 eV is suggested by van der Wiel *et al.*[25] and recent measurements up to 600 eV provide an f sum rule within ~2% of the correct value.[52] The possible small discrepancy between theory and experiment shown in Fig. 4, other than that due to the structure at 23 eV, is presumably accounted for by the contributions of other states in N_2^+ which are neglected in the present calculations. Specifically, the lowest few vibrational levels in the $C^2\Sigma_u^+$ state of N_2^+,[53] which is largely predissociated by the $B^2\Sigma_u^+$ and a $^4\Pi_u$ state, can contribute weakly to the production of N_2^+ ions.[54]

A further comparison between theory and experiment is provided by recent branching-ratio measurements for the production of $X^2\Sigma_g^+$, $A^2\Pi_u$, and $B^2\Sigma_u^+$ states in N_2^+ upon photoionization of N_2.[21,27,28] In Figs. 5 and 6 are shown partial photoionization cross sections for the production of $X^2\Sigma_g^+$, $A^2\Pi_u$, and $B^2\Sigma_u^+$ states in N_2^+, respectively. The theoretical results are obtained from Figs. 1 to 3 and, consequently, correspond to vibrational- and rotational-averaged cross sections. The experimental partial cross sections obtained from electron-scattering measurements[25,27] have been constructed by renormalizing the $(e-2e)$ branching ratios[27] to the total cross sections for N_2^+ production assuming that only the three states considered contribute.[25] By contrast, the partial cross sections cited by Brion, *et al.*,[27] normalized to

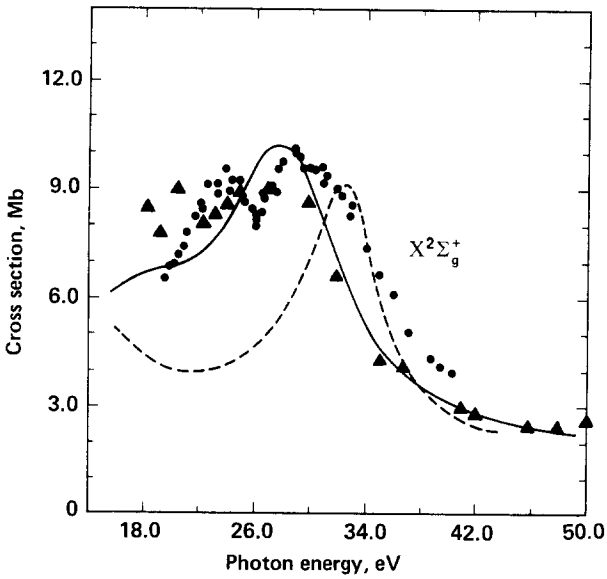

FIG. 5. Partial photoionization cross section in N_2 for the production of $(X^2\Sigma_g^+)N_2^+$ ions; solid line (—) Stieltjes–Tchebycheff results in the static-exchange approximation; circles (●) synchrotron radiation measurements [Refs. 22 and 28]; triangles (▲), electron–electron (Ref. 27) and electron–ion (Ref. 25) coincidence measurements; dashed curve (----) X_α calculations (Ref. 7). Error bars of ±15%–20% are suggested for the experimental values.

the forward-scattering optical cross section,[25] do not sum to the N_2^+ cross section of Fig. 4, although the discrepancy is presumably within the error bars of the measurements. The photon branching-ratio measurements[28] are normalized to the total optical cross section,[22a] both sets of values corresponding to the use of synchrotron radiation. In view of the necessity of deconvoluting photoelectron spectra in each case, the partial cross sections obtained using photons[22,28] and electrons,[25,27] respectively, are in generally good mutual accord, with error bars of approximately ±15%–20% appropriate.[55] The very recently reported branching ratio measurements using a line source are also in good accord with the results of Figs. 5 and 6.[21(c)]

Referring to Fig. 5, the calculations are evidently in excellent agreement with the partial cross sections obtained employing both synchrotron radiation and electron-scattering techniques. The large shape resonance present at ~ 28 eV in this channel accounts for the inflection in the total cross section of Fig. 4. Although the photon and electron results are in good mutual accord,[55] there are differences in structural detail in the 18–26 eV excitation interval. A Rydberg series in this spectral interval converging on the $C^2\Sigma_u^+$ is a possible candidate for these structures,[53] due to autoionization into the $(k\pi_u)X^2\Sigma_g^+$ channel via both configuration interaction and vibronic coupling.[56] The recent X_α results[7(b)] also shown in Fig. 5 predict a shape resonance in this channel which is in qualitative, but not quantitative, accord with the present static-exchange results and the experimental measurements. Similar observations have been made in connection with theoretical studies of the shape resonance in the K-shell photoionization cross section in molecular nitrogen.[7(a),19]

The calculated $B^2\Sigma_u^+$ cross section shown in Fig. 6 is evidently in good agreement with both sets of experimental values, which are in excellent mutual accord, whereas the calculated $A^2\Pi_u$ cross section is in agreement with the measurements at threshold, but falls systematically below experiment at higher excitation energies. The origin of the small discrepancy in the $A^2\Pi_u$ channel can be understood by recognizing that excitations out of the $1\pi_u$ orbital break the cylindrical symmetry of the core and hence it can be expected that orbital relaxation and channel coupling effects, which are not treated in this work, will be more important in this case. Both sets of experimental values for this channel are in good mutual accord,[55] and indicate the presence of an autoionizing feature at ~ 23 eV.[53,54] This structure, and that at 23 eV in the $X^2\Sigma_g^+$ channel (Fig. 5), gives rise to the related feature in the total cross section of Fig. 4. Agreement with the X_α calculations also shown in Fig. 6 is evidently satisfactory.[7(b)]

VI. CONCLUDING REMARKS

Photoabsorption cross-section calculations for molecular nitrogen are reported in the present study employing the recently devised Stieltjes–Tchebycheff moment-theory technique in the separated-channel static-exchange approximation. It is particularly important to emphasize that the moment-theory technique entails the use of only normalizable basis functions, which facilitates the construction of orbitals and many-electron states having the appropriate molecular symmetries. By contrast, attempts to construct separately discrete and continuum functions having the appropriate molecular symmetries can encounter considerable computational difficulties. The Stieltjes–Tchebycheff procedure provides photoionization cross sections equivalent to those obtained using continuum functions, but avoids their explicit construction. Consequently, in contrast to previously reported local or model potential studies, precise evaluations of partial and total photoabsorption

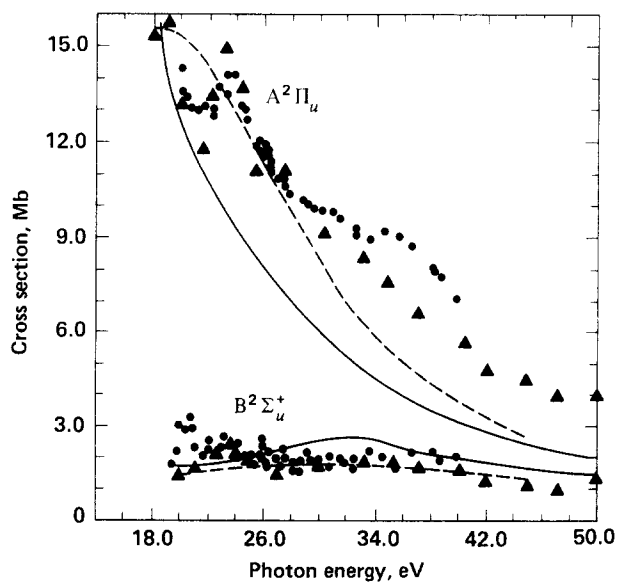

FIG. 6. As in Fig. 5, for the production of $A^2\Pi_u$ (upper curve) and $B^2\Sigma_u^+$ (lower curve) states in N_2^+.

cross sections are achieved in the separated-channel static-exchange approximation in the present development, without further computational approximation. Moreover, the pseudospectrum of functions obtained from the quantum mechanical calculations provides a basis for clarifications of the origins of resonance features present in the cross sections, in accordance with the stabilization phenomenon and the conventional procedures of computational quantum chemistry.

The separated-channel static-exchange calculations reported here evidently provide excellent first approximations to photoabsorption processes in molecular nitrogen. It is particularly satisfying that the results obtained for the $X^2\Sigma_g^+$ channel shown in Fig. 5 are in excellent accord with the measured partial cross section, since this channel is expected *a priori* to couple weakly with other channels. The agreement with experimental values for the $A^2\Pi_u$ and $B^2\Sigma_u^+$ channels shown in Fig. 6 is also satisfactory, as is the agreement for the total cross section shown in Fig. 4. These results suggest that the approach employed here can also provide reliable photoionization cross sections for other diatomic molecules in which channel-coupling effects are small. Consequently, it is desirable to formulate related moment-theory methods for the calculation of distributions of photoejected electrons following recently described procedures,[57] to devise procedures for explicitly introducing the effects of channel coupling, and to include the effects of vibrational motion in such calculations.

ACKNOWLEDGMENTS

The authors acknowledge helpful discussions and correspondence with R. A. Bonham, C. E. Brion, D. C. Cartwright, D. E. Eastman, T. Gustafson, A. U. Hazi, Y.-K. Kim, E. W. Plummer, M. J. van der Wiel, and N. Winter. We also thank W. P. Reinhardt and the JILA Fellows for their kind hospitality to PWL, C. T. Corcoran for computational assistance, and R. H. Garstang and G. B. Ellison for bringing the review of Lofthus and Krupenie to our attention. Acknowledgment is made to the Donors of the Petroleum Research Fund, administered by the American Chemical Society for partial support of these studies.

[1] *Critical Review of Ultraviolet Photoabsorption Cross Sections for Molecules of Astrophysical and Aeronomic Interest*, edited by R. D. Hudson, NSRDS-NBS 38 (U.S. GPO, Washington, DC, 1971).

[2] *Photoionization and Other Probes of Many-Electron Interactions*, edited by F. J. Wuilleumier (Plenum, New York, 1976).

[3] D. R. Bates, J. Chem. Phys. **19**, 1122 (1951); D. R. Bates, U. Öpik, and G. Poots, Proc. Phys. Soc. A **66**, 1113 (1953).

[4] E. J. McGuire, Phys. Rev. **175**, 20 (1968).

[5] H. P. Kelly, Chem. Phys. Lett. **20**, 547 (1973).

[6] F. O. Ellison, J. Chem. Phys. **61**, 507 (1974); J. W. Rabalais, T. P. Debies, J. L. Berkosky, J.-T. J. Huang, and F. O. Ellison, J. Chem. Phys. **61**, 516; 529 (1974).

[7] (a) D. Dill and J. L. Dehmer, J. Chem. Phys. **61**, 692 (1974); J. L. Dehmer and D. Dill, Phys. Rev. Lett. **35**, 213 (1975); J. Chem. Phys. **65**, 5327 (1976); (b) J. W. Davenport, Phys. Rev. Lett. **36**, 945 (1976); Int. J. Quantum Chem. S11, 89 (1977).

[8] B. Schneider and R. S. Berry, Phys. Rev. **182**, 141 (1969); H. C. Tuckwell, J. Phys. B **3**, 293 (1970); S. Iwata and S. Nagukura, Mol. Phys. **27**, 425 (1974); C. Duzy and R. S. Berry, J. Chem. Phys. **64**, 2421 (1976); F. Hirota, J. Electron Spectrosc. Relat. Phenom. **9**, 149 (1976).

[9] Various techniques employing discrete basis functions in photoionization studies have been devised recently, including: analytic continuation methods [J. T. Broad and W. P. Reinhardt, J. Chem. Phys. **60**, 2182 (1974), T. N. Rescigno, C. W. McCurdy, and V. McKoy, Phys. Rev. A **9**, 2409 (1974), P. H. S. Martin, T. N. Rescigno, V. McKoy, and W. H. Henneker, Chem. Phys. Lett. **29**, 496 (1974), M. A. C. Nascimento and W. A. Goddard, Phys. Rev. A. **16**, 1559 (1977)]; J-matrix methods [J. T. Broad and W. P. Reinhardt, J. Phys. B **9**, 1491 (1976)]; equivalent-quadrature methods [H. A. Yamani and W. P. Reinhardt, Phys. Rev. A **11**, 1144 (1975)]; coordinate rotation methods [T. N. Rescigno and V. McKoy, Phys. Rev. A **12**, 522 (1975), T. N. Rescigno, C. W. McCurdy, and V. McKoy, J. Chem. Phys. **64**, 477 (1976)]; Green's function methods [H. Doyle, M. Oppenheimer, and A. Dalgarno, Phys. Rev. A **11**, 909 (1975), M. Oppenheimer and H. Doyle, Phys. Rev. A **13**, 665 (1976)]. Some appropriate intercomparative remarks are given by C. T. Corcoran and P. W. Langhoff, Chem. Phys. Lett. **41**, 609 (1976), and also appear in the references cited in 10 and 11.

[10] (a) P. W. Langhoff, Chem. Phys. Lett. **22**, 60 (1973); (b) P. W. Langhoff and C. T. Corcoran, J. Chem. Phys. **61**, 146 (1974); (c) P. W. Langhoff, J. Sims, and C. T. Corcoran, Phys. Rev. A **10**, 829 (1974).

[11] (a) P. W. Langhoff and C. T. Corcoran, Chem. Phys. Lett. **40**, 367 (1976); (b) P. W. Langhoff, C. T. Corcoran, J. S. Sims, F. Weinhold, and R. M. Glover, Phys. Rev. A **14**, 1042 (1976); (c) C. T. Corcoran and P. W. Langhoff, J. Math. Phys. 18, 651 (1977).

[12] See, for example, H. F. Schaefer III, *The Electronic Structure of Atoms and Molecules* (Addison-Wesley, Reading, MA, 1972); Annu. Rev. Phys. Chem. **27**, 261 (1976).

[13] J. A. Shohat and J. D. Tamarkin, *The Problem of Moments*, *Mathematical Surveys*, 1 (American Mathematical Society, Providence, 1943).

[14] R. F. Stewart, C. Laughlin, and G. A. Victor, Chem. Phys. Lett. **29**, 353 (1974).

[15] P. W. Langhoff, C. T. Corcoran, and J. S. Sims, Phys. Rev. A **16**, 1513 (1977).

[16] R. K. Nesbet, Phys. Rev. A **14**, 1065 (1976).

[17] S. V. O'Neil and W. P. Reinhardt, ERDA Report No. E(49-1)-3800 (1976), Chap. 6.

[18] P. W. Langhoff, S. R. Langhoff, and C. T. Corcoran, J. Chem. Phys. **67**, 1722 (1977).

[19] T. N. Rescigno and P. W. Langhoff, Chem. Phys. Lett. **51**, 65 (1977); T. N. Rescigno, C. F. Bender, and V. McKoy, Phys. Rev. A (to be published); A. U. Hazi and T. N. Rescigno, Phys. Rev. A (to be published).

[20] R. E. Huffman, Y. Tanaka, and J. C. Larrabee, J. Chem. Phys. **39**, 910 (1963); G. R. Cook and P. H. Metzger, J. Chem. Phys. **41**, 321 (1964).

[21] (a) J. A. R. Samson and R. B. Cairns, J. Geophys. Res. **69**, 4583 (1964); J. Opt. Soc. Am. **55**, 1035 (1965); (b) J. W. Rabalais, T. P. Debies, J. L. Berkosky, J.-T. J. Huang, and F. O. Ellison, J. Chem. Phys. **61**, 516 (1974); J. L. Gardner and J. A. R. Samson, J. Chem. Phys. **62**, 1447 (1975); (c) J. A. R. Samson, G. N. Haddad, and J. L. Gardner, J. Phys. B **10**, 1749 (1977).

[22] (a) L. C. Lee, R. W. Carlson, D. L. Judge, and M. Ogawa, J. Quant. Spectrosc. Radiat. Transfer **13**, 1023 (1973); (b) P. Gürtler, V. Saile, and E. E. Koch, Chem. Phys. Lett. **48**, 245 (1977).

[23] A. Lofthus and P. H. Krupenie, J. Phys. Chem. Ref. Data **6**, 113 (1977).

[24] J. S. Lee, T. C. Wong, and R. A. Bonham, J. Chem. Phys. **63**, 1643 (1975).

[25] Th. M. El-Sherbini and M. J. Van der Wiel, Physica **59**, 433

(1972); G. R. Wight, M. J. Van der Wiel, and C. E. Brion, J. Phys. B **9**, 675 (1976).
[26]A. J. Blake and J. H. Carver, J. Chem. Phys. **47**, 1038 (1967). See also D. W. Turner, C. Baker, A. D. Baker, and C. R. Brundle, *Molecular Photoelectron Spectroscopy* (Wiley, New York, 1970).
[27]A. Hamnett, W. Stoll, and C. E. Brion, J. Electron Spectrosc-Relat. Phenom. **8**, 367 (1976).
[28]E. W. Plummer, T. Gustafsson, W. Gudat, and D. E. Eastman, Phys. Rev. A **15**, 2339 (1977).
[29]P. W. Langhoff, J. Chem. Phys. **57**, 2604 (1972).
[30]U. Fano and J. W. Cooper, Rev. Mod. Phys. **40**, 441 (1968).
[31]E. J. Heller, Ph.D. thesis (Harvard University, 1973) (unpublished); see also the discussion in Sec. V in H. A. Yamani and W. P. Reinhardt, Phys. Rev. A **11**, 1144 (1975); and P. L. Altick, Phys. Rev. A **10**, 1003 (1974).
[32]J. T. Broad, Ph.D. thesis (Harvard University, 1975) (unpublished).
[33]The single-channel case is discussed by A. U. Hazi and H. S. Taylor, Phys. Rev. A **2**, 1109 (1970). For discussion of the information content of L^2 solutions obtained from the discretization of a multichannel problem, see A. U. Hazi, Chem. Phys. Lett. **20**, 251 (1973).
[34]Previous applications of the Stieltjes–Tchebycheff procedure to the photoionization of molecular nitrogen in the random-phase approximation indicate the presence of spurious contributions to the total cross section from weakly coupled channels; T. N. Rescigno, C. F. Bender, B. V. McKoy, and P. W. Langhoff (unpublished). Similar observations are made by R. K. Nesbet (Ref. 16) in studies of atomic boron. Note, however, that the pseudospectrum employed in this latter case is a particularly sparse one in the spectral region under study, and consequently is not expected to provide a very smooth continuum profile in any event. Further discussion of the presence of spuriously large structures in photoionization cross sections obtained from the moment approach is given in Refs. 10 and 11.
[35]Moment-theory and L^2 techniques have been employed by P. W. Langhoff, J. S. Sims, and C. T. Corcoran in investigations of autoionization line shapes (unpublished).
[36]H. P. Kelly, Phys. Rev. **136**, B896 (1964).
[37]P. W. Langhoff, M. Karplus, and R. P. Hurst, J. Chem. Phys. **44**, 505 (1966).
[38]W. J. Hunt and W. A. Goddard III, Chem. Phys. Lett. **3**, 414 (1969); Chem. Phys. Lett. **24**, 464 (1974).
[39]P. W. Langhoff and S. W. Chan, Mol. Phys. **25**, 345 (1973).
[40]Photoionization calculations in N_2 employing configuration-interaction techniques and the Stieltjes–Tchebycheff method are currently in progress; S. V. O'Neil and W. P. Reinhardt (private communication).
[41]M. E. Riley and D. G. Truhlar, J. Chem. Phys. **65**, 792 (1976).
[42]T. H. Dunning, J. Chem. Phys. **53**, 2823 (1970).
[43]P. E. Cade, K. D. Sales, and A. C. Wahl, J. Chem. Phys. **44**, 1973 (1966).
[44]H. S. Wall, *Analytic Theory of Continued Fractions* (Van Nostrand, New York, 1948), p. 209.
[45]R. S. Mulliken, in *The Threshold of Space*, edited by M. Zelikoff (Pergamon, New York, 1957), p. 169.
[46]R. S. Mulliken, J. Chem. Phys. **7**, 14 (1939); R. S. Mulliken and C. A. Rieke, Rep. Prog. Phys. **8**, 231 (1941).
[47]R. S. Mulliken, Chem. Phys. Lett. **25**, 305 (1974); **46**, 197 (1977).
[48]R. S. Mulliken, Acc. Chem. Res. **9**, 7 (1976).
[49]G. Herzberg, *Spectra of Diatomic Molecules* 2nd ed. (Van Nostrand, New York, 1950).
[50]F. R. Gilmore, J. Quant. Spectrosc. Radiat. Transfer **5**, 369 (1965).
[51]D. L. Albritton, A. L. Schmeltekopf, and R. N. Zare, *Diatomic Intensity Factors* (Harper and Row, New York, 1977).
[52]R. B. Kay, Ph. E. Van der Leeuw, and M. J. van der Wiel, J. Phys. B 10, 2513 (1977).
[53]K. Codling, Astrophys. J. **143**, 552 (1966).
[54]J. C. Lorquet and M. Desouter, Chem. Phys. Lett. **16**, 136 (1972); C. A. Van der Runstraat, F. J. De Heer, and T. R. Govers, Chem. Phys. **3**, 431 (1974); A. L. Roche and H. Lefebvne-Brion, Chem. Phys. Letters **32**, 155 (1975); D. C. Cartwright and T. H. Dunning, J. Phys. B **8**, L100 (1975).
[55]Although the respective error bars for the partial cross sections of Figs. 5 and 6 obtained from the electron and photon measurements overlap, there is a discernable discrepancy in the respective mean values above 30 eV. This discrepancy is discussed in considerable detail by E. W. Plummer *et al.* (Ref. 28), and can be accounted for by noting that the synchrotron radiation branching ratios for the X, A, and B states sum to 100% (Fig. 8, Ref. 28), indicating that higher-lying states do not contribute significantly to the synchrotron radiation measurements. By contrast, the $(e, 2e)$ measurements indicate non-negligible contributions from higher states above[25] ~ 30 eV excitation energy. When the branching ratio obtained from the synchrotron radiation measurements are renormalized to the fraction of the optical cross section corresponding to N_2^+ production [Ref. 25], the mean values of the photon and electron partial cross sections are in good accord. Of course corrections due to anisotropy effects can also contribute to the discrepancy, although these are apparently small in the case of molecular nitrogen. Y.-K. Kim (private communication) has noted that when the total synchrotron cross section data [Ref. 22(a)] is examined on a Platzman plot, there is an irregular broad feature present in the 30–40 eV region, with the values lying above the line source measurements [Ref. 21a] and the electron scattering data (Refs. 24 and 25). A similar feature is apparently present in the partial photoionization cross sections obtained from the synchrotron measurements, and is particularly noticable in the $A\,^2\Pi_u$ channel of Fig. 6. Note, however, that when the appropriate error bars of the various photon (Refs. 21, 22, and 28) and electron (Refs. 24, 25, and 27) measurements are taken into account, the results are in mutual accord. We are grateful to Y.-K. Kim for his helpful remarks, and to C. E. Brion, D. E. Eastman, T. Gustafson, E. W. Plummer, and M. J. van der Wiel, for correspondence and for providing preprints of their work.
[56]Recent high resolution time-of-flight [R. E. Kennerly, Rev. Sci. Instrum. **48**, 48 (1977)], threshold-photoelectron-spectroscopy by electron-attachment [A. Chutjian and J. M. Ajello, J. Chem. Phys. **65**, 5524 (1977) and photon [G. V. Marr and P. R. Woodruff, J. Phys. B **9**, L377 (1976)] and electron [D. G. Wilden, P. J. Hicks, and J. Comer, J. Phys. B **9**, 1959 (1976)] branching ratio measurements should aid in clarifying the origins of the various structures in the N_2 spectra due to autoionization. See also, J. Berkowitz and W. A. Chupka, J. Chem. Phys. **51**, 2341 (1969). For a recent theoretical discussion treating the spectral region between the X and A states in N_2^+ (15.6–16.9 eV), see C. Duzy and R. S. Berry, J. Chem. Phys. **64**, 2431 (1976).
[57]C. W. McCurdy, T. N. Rescigno, and V. McKoy, J. Phys. B **9**, 691 (1976); T. N. Rescigno, C. F. Bender, C. W. McCurdy, and V. McKoy, J. Phys. B **9**, 2141 (1976). See also, J. Tully, R. S. Berry, and B. J. Dalton, Phys. Rev. **176**, 95 (1968).